Hindawi
Mathematical Problems in Engineering
Volume 2020, Article ID 6978329, 14 pages
https://doi.org/10.1155/2020/6978329

Research Article

Research on Transmission Characteristics of Hydromechanical Continuously Variable Transmission of Tractor

Junyan Wang,[1,2] Changgao Xia,[1] Xin Fan,[1,3] and Junyu Cai[1]

[1]*School of Automotive and Traffic Engineering, Jiangsu University, Zhenjiang 212013, China*
[2]*School of Transportation, Zhenjiang College, Zhenjiang 212028, China*
[3]*School of Automobile and Traffic Engineering, Jiangsu University of Technology, Changzhou 213001, China*

Correspondence should be addressed to Changgao Xia; xiacg@ujs.edu.cn

Received 9 January 2020; Accepted 13 June 2020; Published 12 August 2020

Academic Editor: Giorgio Besagni

This paper proposes a new transmission scheme of hydromechanical continuously variable transmission (HMCVT) for tractors. The HMCVT has 4 working ranges in each of the front and rear directions. The speed characteristic and the torque characteristic of HMCVT are theoretically derived. On the basis of HMCVT power flow direction, the Крейнес formula is used to calculate the transmission efficiency. Then, the image analysis method is used to study the influence of parameters on the transmission efficiency of HMCVT, and the main influencing factors are found. The results of theoretical derivation demonstrate that, by coordinating control of the HST displacement ratio and the engagement conditions of shifting clutches, the stepless speed regulation of HMCVT at the tractor speed of 0–50 km/h can be realized. The proposed HMCVT has the ability to continuously transmit and change torque over all working ranges. The overall transmission efficiency of HMCVT is at a high level. To verify the theoretical derivation, Amesim simulation software is used for the modeling and simulation of HMCVT. The simulation results are consistent with the theoretical analysis results. Therefore, the HMCVT proposed in this paper has the advantages of compact structure and high transmission efficiency, and it is suitable for matching tractors.

1. Introduction

In addition to transportation, the main function of tractors is to drive agricultural machinery needed for agricultural production, which needs the transmission of tractors to provide constantly changing speed and torque to adapt to frequent external load changes [1].

In this context, the use of a continuously variable transmission (CVT) for tractors has become a trend. The most common type of CVTs is the hydraulic static transmission (HST) [2]; it mainly includes hydraulic pumps, hydraulic motors, and control mechanism. HST has good performance at low speed and can easily switch between positive rotation and negative rotation. However, its transmission efficiency is much lower than that of gear transmission, which leads to the fact that it is rarely used in tractors.

In order to overcome the above shortcomings, the HST is connected in parallel with the mechanical components to form a hydromechanical continuously variable transmission (HMCVT) [3–6]. HMCVT transmits only part of the power through the HST; the remaining power is transmitted through the mechanical components, so the efficiency is much higher than HST. HMCVT can realize stepless speed regulation through the HST, while relying on mechanical components to achieve high efficiency transmission. In addition, the HMCVT can control the engine to operate on an optimal power curve or optimal economic curve, thus achieving optimum power performance or optimum fuel economy for tractors [7–9].

The research on power split continuously variable transmission technology began in the early 20th century in the world. However, limited by the level of hydraulic system manufacturing, this type of transmission was not used in

armored and heavy construction vehicles until the late 1960s [10]. Literature [8] first proposes a transmission scheme for single-row planetary gears with two hydromechanical working ranges. In each of the two working ranges, the maximum speed of the tractor can reach 32 km/h and 50 km/h, respectively. Then, according to the market demand, only one hydromechanical working range transmission scheme is proposed, which can match the 75 kw engine. The forward driving speed is from 0 to 40 km/h, and the reverse driving speed is from 0 to 25 km/h [11]. The transmission developed by Steyr company has three planetary gear rows, controlled by 4 clutches and 2 brakes. This transmission can achieve speed adjustments from 0 to 50 km/h [12]. The authors of [13, 14] study a HMCVT that has four planetary gear rows and can achieve speed adjustment from 0 to 40 km/h. The author of [15] proposes a transmission scheme in which a single-row planetary gear is connected in series with a mechanical stepped transmission. This transmission has 6 ranges in the forward direction and 3 ranges in the reverse direction.

In general, the more the transmission ranges, the greater the expansion of the hydraulic power [10], but it will lead to frequent switching during the ranges and reducing the transmission performance. The single-row planetary scheme helps to reduce the size of the transmission, but the hydraulic motor needs to be reversed quickly at the moment of switching, which needs high performance of the hydraulic motor.

This paper will propose a transmission scheme for a new 4-range HMCVT suitable for wheeled tractors and then conduct a detailed theoretical analysis on the transmission characteristics (speed characteristic, torque characteristic, and efficiency characteristic) of HMCVT and find out the important factors that affect the efficiency of HMCVT; finally, the Amesim simulation software is used to verify the transmission scheme.

2. Transmission Scheme of HMCVT

The structure of HMCVT proposed in this paper is shown in Figure 1. It includes the input shaft, pump-motor hydraulic system, planetary gear mechanism, gear pairs, shifting clutches, and directional clutches. The hydraulic path of HMCVT is the HST, and its mechanical path is the Ravigneaux planetary gear mechanism (PGM). The hydraulic path and the mechanical path are connected in parallel to form a closed loop and then are connected in series with the range switching mechanism. In the PGM, when the output component is the carrier c, it is an ordinary PGM; when the output component is the small sun gear s_2, then it is a Ravigneaux PGM. In addition, part of the engine power is through the HST into the PGM, and the HST realizes the stepless transmission.

There are 6 clutches in the HMCVT, which are 4 shifting clutches and 2 directional clutches. Different clutches can realize 4 working ranges in the front or rear directions. In order to ensure that engine power can be transferred from the input shaft to the output shaft, one shifting clutch and one directional clutch must be engaged. The engagement conditions of clutches in each range of HMCVT are shown in Table 1.

3. Theoretical Analysis on Transmission Characteristics of HMCVT

3.1. Speed Characteristic

3.1.1. Ranges HM1 and HM3. The power transmission routes of ranges HM_1 and HM_3 are basically the same, except for the difference between gear pairs i_7 and i_8. Under these two conditions, the power is input by the large sun gear s_1 and the ring gear r and output by the carrier c.

If n_e denotes the engine speed, the variable pump input shaft speed n_p is

$$n_p = \frac{n_e}{(i_1 i_2)}. \tag{1}$$

Ignoring the effect of the volumetric efficiency of the volumetric speed control loop, the relationship between the motor output shaft speed n_m, the variable pump input shaft speed n_p, and the pump-motor displacement ratio ε is

$$n_m = \varepsilon n_p = \frac{\varepsilon n_e}{i_1 i_2}, \tag{2}$$

where $\varepsilon = Q_p/Q_m - 1 \le \varepsilon \le 1$, Q_p is the displacement of the variable pump, and Q_m is the displacement of the quantitative motor.

The input speed of the large sun gear in PGM n_{s_1} is

$$n_{s1} = \frac{n_m}{(-i_3)} = \frac{\varepsilon n_e}{-i_1 i_2 i_3}. \tag{3}$$

The input speed of the ring gear n_r equals n_e. According to the PGM speed characteristic formula [16], the relationship between the input speed of large sun gear n_{s_1}, the input speed of ring gear n_r, the output speed of carrier n_c, and the PGM standing transmission ratio $-k_1$ is satisfied:

$$n_{s_1} - k_1 n_r - (1 - k_1) n_c = 0, \tag{4}$$

where $-k_1 = Z_r/Z_{s_1} > 1$, Z_r is the number of teeth of the ring gear, and Z_{s_1} is the number of teeth of the large sun gear.

Therefore, the output speed of the carrier n_c is

$$n_c = \frac{-k_1 i_1 i_2 i_3 - \varepsilon}{(1 - k_1) i_1 i_2 i_3} n_e. \tag{5}$$

The intermediate shaft speed n_z is

$$n_z = \begin{cases} \dfrac{-k_1 i_1 i_2 i_3 - \varepsilon}{(1 - k_1) i_1 i_2 i_3 i_4 i_8} n_e, & (HM_1), \\[2ex] \dfrac{-k_1 i_1 i_2 i_3 - \varepsilon}{(1 - k_1) i_1 i_2 i_3 i_4 i_7} n_e, & (HM_3). \end{cases} \tag{6}$$

Finally, the output shaft speed of HMCVT n_o is

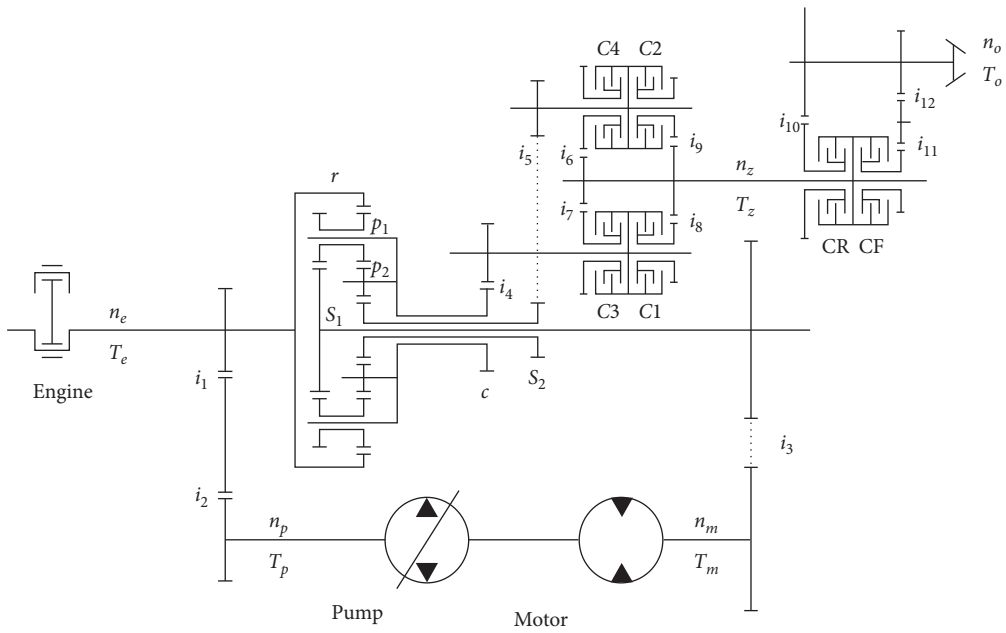

Figure 1: The structure of HMCVT.

Table 1: Engagement conditions of clutches of HMCVT.

Range		Directional clutch		Shifting clutch			
		CF	CR	C1	C2	C3	C4
Forward	First	+		+			
	Second	+			+		
	Third	+				+	
	Fourth	+					+
Reverse	First		+	+			
	Second		+		+		
	Third		+			+	
	Fourth		+				+

$$n_o = \begin{cases} \dfrac{-k_1 i_1 i_2 i_3 - \varepsilon}{(1-k_1) i_1 i_2 i_3 i_4 i_8 i_{11} i_{12}} n_e, & (HM_1), \\ \dfrac{-k_1 i_1 i_2 i_3 - \varepsilon}{(1-k_1) i_1 i_2 i_3 i_4 i_7 i_{11} i_{12}} n_e, & (HM_3). \end{cases} \tag{7}$$

The transmission ratio of HMCVT i_g is

$$i_g = \frac{n_e}{n_o} = \begin{cases} \dfrac{(1-k_1) i_1 i_2 i_3 i_4 i_8 i_{11} i_{12}}{-k_1 i_1 i_2 i_3 - \varepsilon}, & (HM_1), \\ \dfrac{(1-k_1) i_1 i_2 i_3 i_4 i_7 i_{11} i_{12}}{-k_1 i_1 i_2 i_3 - \varepsilon} & (HM_3). \end{cases} \tag{8}$$

3.1.2. Ranges HM2 and HM4. The power transmission routes of ranges HM_2 and HM_4 are the same, except for the difference between gear pairs i_6 and i_9. Under these two conditions, the power is input by the large sun gear s_1 and the ring gear r and output by the small sun gear s_2.

The same as the previous case, the input speed of the large sun gear n_{s_1} is $n_{s_1} = -\varepsilon n_e / (i_1 i_2 i_3)$; the input speed of the ring gear n_r equals n_e. According to the PGM speed characteristic formula (16), the relationship between the input speed of large sun gear n_{s_1}, the input speed of ring gear n_r, the output speed of the small sun gear n_{s_2}, and the PGM standing transmission ratios k_2 and $-k_3$ is satisfied:

$$\frac{1-k_3}{k_2-k_3} n_r - \frac{1-k_2}{k_2-k_3} n_{s_1} - n_{s_2} = 0. \tag{9}$$

Therefore, the output speed of the small sun gear n_{s_2} is

$$n_{s_2} = \frac{(1-k_3) i_1 i_2 i_3 + (1-k_2)\varepsilon}{(k_2-k_3) i_1 i_2 i_3} n_e, \tag{10}$$

where $k_2 = Z_{s_2}/Z_r > 0$, $-k_3 = Z_{s_2}/Z_{s_1} > 0$, and Z_r, Z_{s_1}, Z_{s_2} are the numbers of teeth of ring gear, large sun gear, and small sun gear, respectively.

The intermediate shaft speed n_z is

$$n_z = \begin{cases} \dfrac{(1-k_3)i_1i_2i_3 + (1-k_2)\varepsilon}{(k_2-k_3)i_1i_2i_3i_5i_9} n_e, & (\mathrm{HM}_2), \\ \dfrac{(1-k_3)i_1i_2i_3 + (1-k_2)\varepsilon}{(k_2-k_3)i_1i_2i_3i_5i_6} n_e, & (\mathrm{HM}_4). \end{cases} \tag{11}$$

Finally, the output shaft speed of HMCVT n_o is

$$n_o = \begin{cases} \dfrac{(1-k_3)i_1i_2i_3 + (1-k_2)\varepsilon}{(k_2-k_3)i_1i_2i_3i_5i_9i_{11}i_{12}} n_e, & (\mathrm{HM}_2), \\ \dfrac{(1-k_3)i_1i_2i_3 + (1-k_2)\varepsilon}{(k_2-k_3)i_1i_2i_3i_5i_6i_{11}i_{12}} n_e, & (\mathrm{HM}_4). \end{cases} \tag{12}$$

The transmission ratio of HMCVT i_g is

$$i_g = \frac{n_e}{n_o} = \begin{cases} \dfrac{(k_2-k_3)i_1i_2i_3i_5i_9i_{11}i_{12}}{(1-k_3)i_1i_2i_3 + (1-k_2)\varepsilon}, & (\mathrm{HM}_2), \\ \dfrac{(k_2-k_3)i_1i_2i_3i_5i_6i_{11}i_{12}}{(1-k_3)i_1i_2i_3 + (1-k_2)\varepsilon}, & (\mathrm{HM}_4). \end{cases} \tag{13}$$

3.2. Determination of Parameters of HMCVT. The rated speed of the engine matching with the HMCVT is 2200 r/min, the minimum speed of the tractor is 4 km/h, the maximum speed is 50 km/h, the main reducer ratio of the rear axle is 3.7, the reduction ratio of the wheel side is 5.6, the total transmission ratio of the rear axle is 20.72, and the drive wheel radius is 0.8579 m.

The range of the transmission ratio in the drive train is determined by parameters such as the speed of the tractor, the rated speed of the engine, and the drive wheel radius. So the transmission ratio of each range of HMCVT is calculated as follows:

$$i_{gj} = \frac{0.377 n_e r_d}{v}, \tag{14}$$

where $j = 1, 2, 3, 4$; n_e is the rated speed of the engine; r_d is the drive wheel radius; v is the theoretical driving speed of the tractor.

The HMCVT has 4 working ranges, so the common ratio of the transmission ratios is

$$\varphi = \sqrt[4]{\frac{i_{g\max}}{i_{g\min}}}. \tag{15}$$

The HMCVT adopts a proportional transmission, so, in each working range, the transmission ratio has the following relationship:

$$\frac{i_{gj\max}}{i_{gj\min}} = \varphi. \tag{16}$$

When HMCVT is switching between adjacent ranges, the conditions must be met at the changing point: the transmission ratios are equal and the pump-motor displacement ratios are equal:

$$\begin{cases} i_{g1\min}(-1) = i_{g2\min}(-1), \\ i_{g2\min}(1) = i_{g3\min}(1), \\ i_{g3\min}(-1) = i_{g4\min}(-1), \\ i_{g4\min}(1) = i_{\min}. \end{cases} \tag{17}$$

The gear ratio of the connecting gears between the engine and the hydraulic variable pump needs to be met:

$$i_1 i_2 \geq \frac{n_{e.\max}}{n_{p.\max}}. \tag{18}$$

According to the previous content, if i_{10}, i_{11}, and i_{12} are set to 1, then the relationship between the various parameters of HMCVT can be obtained:

$$\begin{cases} k_1 i_1 i_2 i_3 = -3.2727, \\ 1 - k_3 = k_1(k_2 - 1), \\ i_5 i_6 = \dfrac{0.8969 k_1}{(1+k_1)}, \\ i_4 i_7 = \dfrac{-1.6865 k_1}{(1-k_1)}, \\ i_4 i_8 = \dfrac{-5.9615 k_1}{(1-k_1)}, \\ i_5 i_9 = \dfrac{3.1702 k_1}{(1+k_1)}. \end{cases} \tag{19}$$

These parameters are all expressions about the PGM standing transmission ratio $-k_1$. Once the value of $-k_1$ is determined, the values of these parameters will also be determined, which will be described later.

3.3. Torque Characteristic

3.3.1. Ranges HM1 and HM3. Ignoring the power losses, if T_o denotes the load torque of output shaft, the intermediate shaft torque T_z is

$$T_z = \frac{T_o}{i_{11} i_{12}}, \tag{20}$$

and then the output torque of carrier in PGM T_c is

$$T_c = \begin{cases} \dfrac{T_z}{i_4 i_8} = \dfrac{T_o}{i_4 i_8 i_{11} i_{12}}, & (\mathrm{HM}_1), \\ \dfrac{T_z}{i_4 i_7} = \dfrac{T_o}{i_4 i_7 i_{11} i_{12}}, & (\mathrm{HM}_3). \end{cases} \tag{21}$$

According to the PGM torque characteristic formula (16), the relationship between the input torque of large sun gear T_{s_1}, the input torque of ring gear T_r, the output torque of carrier T_c, and the PGM standing transmission ratio $-k_1$ is satisfied:

$$T_{s_1} = \frac{T_r}{-k_1} = -\frac{T_c}{1-k_1}, \tag{22}$$

where $-k_1 = Z_r/Z_{s_1} > 1$, Z_r is the number of teeth of the ring gear, and Z_{s_1} is the number of teeth of the large sun gear.

Therefore, the large sun gear torque T_{s_1} is

$$T_{s_1} = -\frac{T_c}{1-k_1} = \begin{cases} -\dfrac{T_o}{i_4 i_8 i_{11} i_{12}(1-k_1)}, & (\mathrm{HM}_1), \\ -\dfrac{T_o}{i_4 i_7 i_{11} i_{12}(1-k_1)}, & (\mathrm{HM}_3). \end{cases} \tag{23}$$

Then, the input torque of ring gear T_r is

$$T_r = -k_1 T_{s_1} = \begin{cases} \dfrac{k_1 T_o}{i_4 i_8 i_{11} i_{12}(1-k_1)}, & (\mathrm{HM}_1), \\ \dfrac{k_1 T_o}{i_4 i_7 i_{11} i_{12}(1-k_1)}, & (\mathrm{HM}_3). \end{cases} \tag{24}$$

Thus, the motor shaft load torque T_m is

$$T_m = \frac{T_{s_1}}{-i_3} = \begin{cases} \dfrac{T_o}{i_3 i_4 i_8 i_{11} i_{12}(1-k_1)}, & (\mathrm{HM}_1), \\ \dfrac{T_o}{i_3 i_4 i_7 i_{11} i_{12}(1-k_1)}, & (\mathrm{HM}_3). \end{cases} \tag{25}$$

The pump shaft torque T_p is

$$T_p = \varepsilon T_m = \begin{cases} \dfrac{\varepsilon T_o}{i_3 i_4 i_8 i_{11} i_{12}(1-k_1)}, & (\mathrm{HM}_1), \\ \dfrac{\varepsilon T_o}{i_3 i_4 i_7 i_{11} i_{12}(1-k_1)}, & (\mathrm{HM}_3). \end{cases} \tag{26}$$

The engine output torque T_e is

$$T_e = T_r + \frac{T_p}{i_1 i_2} = \begin{cases} \dfrac{(k_1 i_1 i_2 i_3 + \varepsilon) T_o}{i_1 i_2 i_3 i_4 i_8 i_{11} i_{12}(1-k_1)}, & (\mathrm{HM}_1), \\ \dfrac{(k_1 i_1 i_2 i_3 + \varepsilon) T_o}{i_1 i_2 i_3 i_4 i_7 i_{11} i_{12}(1-k_1)}, & (\mathrm{HM}_3). \end{cases} \tag{27}$$

Finally, the ratio of the output torque of HMCVT to the input torque of the engine μ is

$$\mu = \frac{T_o}{T_e} = \begin{cases} \dfrac{(1-k_1 i_1 i_2 i_3 i_4 i_8 i_{11} i_{12}}{\varepsilon + k_1 i_1 i_2 i_3}, & (\mathrm{HM}_1), \\ \dfrac{(1-k_1) i_1 i_2 i_3 i_4 i_7 i_{11} i_{12}}{\varepsilon + k_1 i_1 i_2 i_3}, & (\mathrm{HM}_3). \end{cases} \tag{28}$$

3.3.2. Ranges HM2 and HM4. The same as the previous case, T_o denotes the load torque of output shaft, and the intermediate shaft torque T_z is $T_z = T_o/(i_{11} i_{12})$. Then the output torque of small sun gear in PGM T_{s_2} is

$$T_{s_2} = \begin{cases} \dfrac{T_z}{i_5 i_9} = \dfrac{T_o}{i_5 i_9 i_{11} i_{12}}, & (\mathrm{HM}_2), \\ \dfrac{T_z}{i_5 i_6} = \dfrac{T_o}{i_5 i_6 i_{11} i_{12}}, & (\mathrm{HM}_4). \end{cases} \tag{29}$$

The external torque algebra sum of PGM is zero, so $T_{s_1} + T_r + T_{s_2} = 0$. According to the PGM torque characteristic formula (16), the relationship between the input torque of large sun gear T_{s_1}, the output torque of small sun gear T_{s_2}, and the PGM standing transmission ratios k_2 and $-k_3$ is satisfied:

$$T_{s_1} = \frac{k_2 - 1}{k_3 - k_2} T_{s_2} = \begin{cases} \dfrac{(k_2-1) T_o}{(k_3-k_2) i_5 i_9 i_{11} i_{12}}, & (\mathrm{HM}_2), \\ \dfrac{(k_2-1) T_o}{(k_3-k_2) i_5 i_6 i_{11} i_{12}}, & (\mathrm{HM}_4). \end{cases} \tag{30}$$

The engine output torque T_e is

$$T_e = \begin{cases} \dfrac{(1-k_2)\varepsilon + (1-k_3) i_1 i_2 i_3}{(k_3-k_2) i_1 i_2 i_3 i_5 i_9 i_{11} i_{12}} T_o, & (\mathrm{HM}_2), \\ \dfrac{(1-k_2)\varepsilon + (1-k_3) i_1 i_2 i_3}{(k_3-k_2) i_1 i_2 i_3 i_5 i_6 i_{11} i_{12}} T_o, & (\mathrm{HM}_4). \end{cases} \tag{31}$$

Finally, the ratio of the output torque of HMCVT to the input torque of the engine μ is

$$\mu = \frac{T_o}{T_e} = \begin{cases} \dfrac{(k_3-k_2) i_1 i_2 i_3 i_5 i_9 i_{11} i_{12}}{(1-k_2)\varepsilon + (1-k_3) i_1 i_2 i_3}, & (\mathrm{HM}_2), \\ \dfrac{(k_3-k_2) i_1 i_2 i_3 i_5 i_6 i_{11} i_{12}}{(1-k_2)\varepsilon + (1-k_3) i_1 i_2 i_3}, & (\mathrm{HM}_4). \end{cases} \tag{32}$$

3.4. Circulating Power Flow Calculation

3.4.1. Ranges HM1 and HM3. The speed ratio of the power transmitting from the engine to the carrier i_{ce} is

$$i_{ce} = \frac{n_c}{n_e} = \frac{-k_1 i_1 i_2 i_3 - \varepsilon}{(1-k_1) i_1 i_2 i_3} = i_{ce}^{r} + i_{ce}^{s_1}. \tag{33}$$

The speed ratios of the power transmitting from the engine to the large sun gear and ring gear $i_{re}/i_{s_1 e}$ are

$$\begin{aligned} i_{re} &= 1, \\ i_{s_1 e} &= -\frac{\varepsilon}{i_1 i_2 i_3}. \end{aligned} \tag{34}$$

In the PGM, the speed ratios between the input elements (large sun gear s_1 and ring gear r) and the output element (carrier c) are

$$i_{cs_1}^{r} = \frac{n_c}{n_{s_1}} = \frac{1}{1-k_1},$$
$$i_{cr}^{s_1} = \frac{n_c}{n_r} = -\frac{k_1}{1-k_1}. \tag{35}$$

Then, we can get

$$i_{ce}^{r} = i_{cs_1}^{r} i_{s_1 e} = -\frac{\varepsilon}{i_1 i_2 i_3 (1-k_1)},$$
$$i_{ce}^{s_1} = i_{cr}^{s_1} i_{re} = -\frac{k_1}{1-k_1}. \tag{36}$$

Next two situations will be discussed as follows [17]:

(1) When $\varepsilon < 0$, $i_{ce}^{s_1} > 0$, $i_{ce}^{r} > 0$, and $i_{ce}^{s_1} i_{ce}^{r} > 0$, the PGM has no circulating power $P_L = 0$.

(2) When $\varepsilon > 0$, $i_{ce}^{s_1} > 0$, $i_{ce}^{r} < 0$, and $i_{ce}^{s_1} i_{ce}^{r} < 0$, the PGM has circulating power; substituting equation (19) for $k_1 i_1 i_2 i_3$ in equation (33), i_{ce} is

$$i_{ce} = \frac{3.2727 - \varepsilon}{3.2727 + i_1 i_2 i_3} > 0. \tag{37}$$

Because of $P_e > 0$, $P_r = (i_{ce}^{s_1}/i_{ce})P_e > 0$, $P_{s_1} = (i_{ce}^{r}/i_{ce})P_e < 0$, the output power P is

$$P = P_e = -P_c = P_r + P_{s_1} = P_r - \left|P_{s_1}\right|. \tag{38}$$

Then,

$$P_r = P + \left|P_{s_1}\right| = P + \left|P_L\right|. \tag{39}$$

The circulating power P_L is

$$P_L = P_{s_1} = \frac{i_{ce}^{r}}{i_{ce}} P_e. \tag{40}$$

Assume that the closed power factor K_L is

$$K_L = \frac{\left|P_L\right|}{P_e} = \left|\frac{i_{ce}^{r}}{i_{ce}}\right| = \left|\frac{\varepsilon}{k_1 i_1 i_2 i_3 + \varepsilon}\right| = |\phi(\varepsilon)|, \tag{41}$$

where $\phi(\varepsilon) = \varepsilon/k_1 i_1 i_2 i_3 + \varepsilon$ and the derivative of $\phi(\varepsilon)$ is $\mathrm{d}\phi(\varepsilon)/\mathrm{d}\varepsilon = k_1 i_1 i_2 i_3/(k_1 i_1 i_2 i_3 + \varepsilon)^2 < 0$, so function $\phi(\varepsilon)$ is a monotonically decreasing function. Then $K_L(0) = 0$, $K_L(1) = 0.44$, and the maximum value of the circulating power is $0.44P_e$.

3.4.2. Ranges HM2 and HM4. The speed ratio of the power transmitting from the engine to the small sun gear $i_{s_2 e}$ is

$$i_{s_2 e} = \frac{n_{s_2}}{n_e} = \frac{(1-k_3) i_1 i_2 i_3 + (1-k_2)\varepsilon}{(k_2 - k_3) i_1 i_2 i_3} = i_{s_2 e}^{r} + i_{s_2 e}^{s_1}. \tag{42}$$

The speed ratios of the power transmitting from the engine to the large sun gear and ring gear $i_{re}/i_{s_1 e}$ are

$$i_{re} = 1,$$
$$i_{s_1 e} = -\frac{\varepsilon}{i_1 i_2 i_3}. \tag{43}$$

In the PGM, the speed ratios between the input elements (large sun gear s_1 and ring gear r) and the output element (small sun gear s_2) are

$$i_{s_2 s_1}^{r} = \frac{k_2 - 1}{k_2 - k_3},$$
$$i_{s_2 r}^{s_1} = \frac{1 - k_3}{k_2 - k_3}. \tag{44}$$

Then, we can get

$$i_{s_2 e}^{r} = i_{s_2 s_1}^{r} i_{s_1 e} = -\frac{(k_2 - 1)\varepsilon}{i_1 i_2 i_3 (k_2 - k_3)},$$
$$i_{s_2 e}^{s_1} = i_{s_2 r}^{s_1} i_{re} = \frac{1 - k_3}{k_2 - k_3}. \tag{45}$$

Next two situations will be discussed as follows [17]:

(1) When $\varepsilon < 0$, $i_{s_2 e}^{s_1} > 0$, $i_{s_2 e}^{r} < 0$, and $i_{s_2 e}^{s_1} i_{s_2 e}^{r} < 0$, the PGM has circulating power; substituting equation (19) for $k_2, k_3, i_1 i_2 i_3$ in equation (42), $i_{s_2 e}$ is

$$i_{s_2 e} = \frac{3.2727 + \varepsilon}{3.2727 - 3.2727/(-k_1)} > 0. \tag{46}$$

Because of $P_e > 0$, $P_r = i_{ce}^{s_1}/i_{ce} P_e > 0$, $P_{s_1} = i_{ce}^{r}/i_{ce} P_e < 0$, the output power P is

$$P = P_e = -P_{s_2} = P_r + P_{s_1} = P_r - \left|P_{s_1}\right|. \tag{47}$$

Then,

$$P_r = P + \left|P_{s_1}\right| = P + \left|P_L\right|. \tag{48}$$

The circulating power P_L is

$$P_L = P_{s1} = \frac{i_{s_2 e}^{r}}{i_{s_2 e}} P_e. \tag{49}$$

Assume that the closed power factor K_L is

$$K_L = \frac{\left|P_L\right|}{P_e} = \left|\frac{i_{s_2 e}^{r}}{i_{s_2 e}}\right| = \left|\frac{-\varepsilon}{k_1 i_1 i_2 i_3 - \varepsilon}\right| = |\phi(\varepsilon)|, \tag{50}$$

where $\phi(\varepsilon) = -\varepsilon/k_1 i_1 i_2 i_3 - \varepsilon$ and the derivative of $\phi(\varepsilon)$ is $\mathrm{d}\phi(\varepsilon)/\mathrm{d}\varepsilon = -k_1 i_1 i_2 i_3/(k_1 i_1 i_2 i_3 - \varepsilon)^2 > 0$, so function $\phi(\varepsilon)$ is a monotonically increasing function. Then, $K_L(0) = 0$, $K_L(1) = 0.44$, and the maximum value of the circulating power is $0.44P_e$.

(2) When $\varepsilon > 0$, $i_{s_2 e}^{s_1} > 0$, $i_{s_2 e}^{r} > 0$, and $i_{s_2 e}^{s_1} i_{s_2 e}^{r} > 0$, the PGM has no circulating power $P_L = 0$.

3.5. Hydraulic Split Power Calculation. Hydraulic power-split ratio $\rho = P_H/P_e = P_{s_1}/P_e$; hydraulic power is input to the PGM through the large sun gear s_1.

3.5.1. Ranges HM1 and HM3

$$\rho = \frac{P_{s_1}}{P_e} = \frac{i_{ce}^r}{i_{ce}} = \frac{\varepsilon}{k_1 i_1 i_2 i_3 + \varepsilon} = \phi(\varepsilon), \tag{51}$$

and as can be obtained from the above, function $\phi(\varepsilon)$ is a monotonically decreasing function, so

$$\begin{cases} \rho(-1) = 0.234 > 0, \\ \rho(0) = 0, \\ \rho(1) = -0.44 < 0. \end{cases} \tag{52}$$

3.5.2. Ranges HM2 and HM4

$$\rho = \frac{P_{s_1}}{P_e} = \frac{i_{s_2 e}^r}{i_{s_2 e}} = \frac{-\varepsilon}{k_1 i_1 i_2 i_3 - \varepsilon} = \phi(\varepsilon). \tag{53}$$

As can be obtained from the above, function $\phi(\varepsilon)$ is a monotonically increasing function, so

$$\begin{cases} \rho(-1) = -0.44 < 0, \\ \rho(0) = 0, \\ \rho(1) = 0.234 > 0. \end{cases} \tag{54}$$

According to the theoretical analysis on the circulating power flow and the hydraulic split power, the power flow direction of HMCVT in each working range is shown in Figure 2. This result lays the foundation for the analysis on the efficiency characteristic of HMCVT.

3.6. Efficiency Characteristic. The Крейнес formula (17) is used to calculate the transmission efficiency of HMCVT:

$$\eta = -\frac{\tilde{\mu}}{i_g} = -\frac{T_o/T_e}{n_e/n_o}, \tag{55}$$

where $\tilde{\mu}$ is the ratio of output torque to input torque of HMCVT considering power losses and i_g is the transmission ratio of HMCVT.

The transmission efficiency calculation process of each working range of HMCVT is shown in Tables 2 and 3. Among them, the calculation processes of the first range and the third range are listed in Table 2, and the calculation processes of the second range and the fourth range are listed in Table 3. In Tables 2 and 3, $i_1 - i_{12}$ are the gear ratios of the gear pairs, $\eta_1 - \eta_{12}$ are the transmission efficiency of the gear pairs, η_H is the hydraulic system transmission efficiency, and $\eta_{s_1 r}$, $\eta_{s_1 s_2}$, and $\eta_{r s_2}$ are the transmission efficiencies of the large sun gear to the ring gear, the large sun gear to the small sun gear, and the ring gear to the small sun gear in the PGM, respectively.

4. Analysis on the Influence of Parameters on the Transmission Efficiency of HMCVT

The results of the transmission efficiency in each working range of HMCVT are as follows:

$$\begin{aligned}
\eta_{HM_1} &= \begin{cases} \dfrac{(\eta_{s_1 r} - k_1)\eta_4\eta_8\eta_{11}\eta_{12}(\varepsilon + k_1 i_1 i_2 i_3)}{(1-k_1)(\eta_1\eta_2\eta_3\eta_H\eta_{s_1 r}\varepsilon + k_1 i_1 i_2 i_3)}, & (\varepsilon > 0), \\[2ex] \dfrac{(\eta_{s_1 r} - k_1)\eta_1\eta_2\eta_3\eta_H\eta_4\eta_8\eta_{11}\eta_{12}(\varepsilon + k_1 i_1 i_2 i_3)}{(1-k_1)(i_1 i_2 i_3\eta_1\eta_2\eta_3\eta_H k_1 + \varepsilon\eta_{s_1 r})}, & (\varepsilon \le 0), \end{cases} \\
\eta_{HM_2} &= \begin{cases} \dfrac{(k_3\eta_{s_1 s_2} - k_2\eta_{r s_2})\eta_5\eta_9\eta_{11}\eta_{12}[(1-k_3)i_1 i_2 i_3 + (1-k_2)\varepsilon]}{(k_3-k_2)[(1-k_3\eta_{s_1 s_2})i_1 i_2 i_3 - \eta_1\eta_2\eta_3\eta_H\varepsilon(k_2\eta_{r s_2} - 1)]}, & (\varepsilon < 0), \\[2ex] \dfrac{(k_3\eta_{s_1 s_2} - k_2\eta_{r s_2})\eta_1\eta_2\eta_3\eta_5\eta_9\eta_{11}\eta_{12}\eta_H[(1-k_3)i_1 i_2 i_3 + (1-k_2)\varepsilon]}{(k_3-k_2)[(1-k_3\eta_{s_1 s_2})i_1 i_2 i_3\eta_1\eta_2\eta_3\eta_H - \varepsilon(k_2\eta_{r s_2} - 1)]}, & (\varepsilon \ge 0), \end{cases} \\
\eta_{HM_3} &= \begin{cases} \dfrac{(\eta_{s_1 r} - k_1)\eta_4\eta_7\eta_{11}\eta_{12}(\varepsilon + k_1 i_1 i_2 i_3)}{(1-k_1)(\eta_1\eta_2\eta_3\eta_H\eta_{s_1 r}\varepsilon + k_1 i_1 i_2 i_3)}, & (\varepsilon > 0), \\[2ex] \dfrac{(\eta_{s_1 r} - k_1\eta_1\eta_2\eta_3\eta_H\eta_4\eta_7\eta_{11}\eta_{12}(\varepsilon + k_1 i_1 i_2 i_3)}{(1-k_1)(i_1 i_2 i_3\eta_1\eta_2\eta_3\eta_H k_1 + \varepsilon\eta_{s_1 r})}, & (\varepsilon \le 0), \end{cases} \\
\eta_{HM_4} &= \begin{cases} \dfrac{(k_3\eta_{s_1 s_2} - k_2\eta_{r s_2})\eta_5\eta_6\eta_{11}\eta_{12}[(1-k_3)i_1 i_2 i_3 + (1-k_2)\varepsilon]}{(k_3-k_2)[(1-k_3\eta_{s_1 s_2})i_1 i_2 i_3 - \eta_1\eta_2\eta_3\eta_H\varepsilon(k_2\eta_{r s_2} - 1)]}, & (\varepsilon < 0), \\[2ex] \dfrac{(k_3\eta_{s_1 s_2} - k_2\eta_{r s_2})\eta_1\eta_2\eta_3\eta_5\eta_6\eta_{11}\eta_{12}\eta_H[(1-k_3)i_1 i_2 i_3 + (1-k_2)\varepsilon]}{(k_3-k_2)[(1-k_3\eta_{s_1 s_2})i_1 i_2 i_3\eta_1\eta_2\eta_3\eta_H - \varepsilon(k_2\eta_{r s_2} - 1)]}, & (\varepsilon \ge 0). \end{cases}
\end{aligned} \tag{56}$$

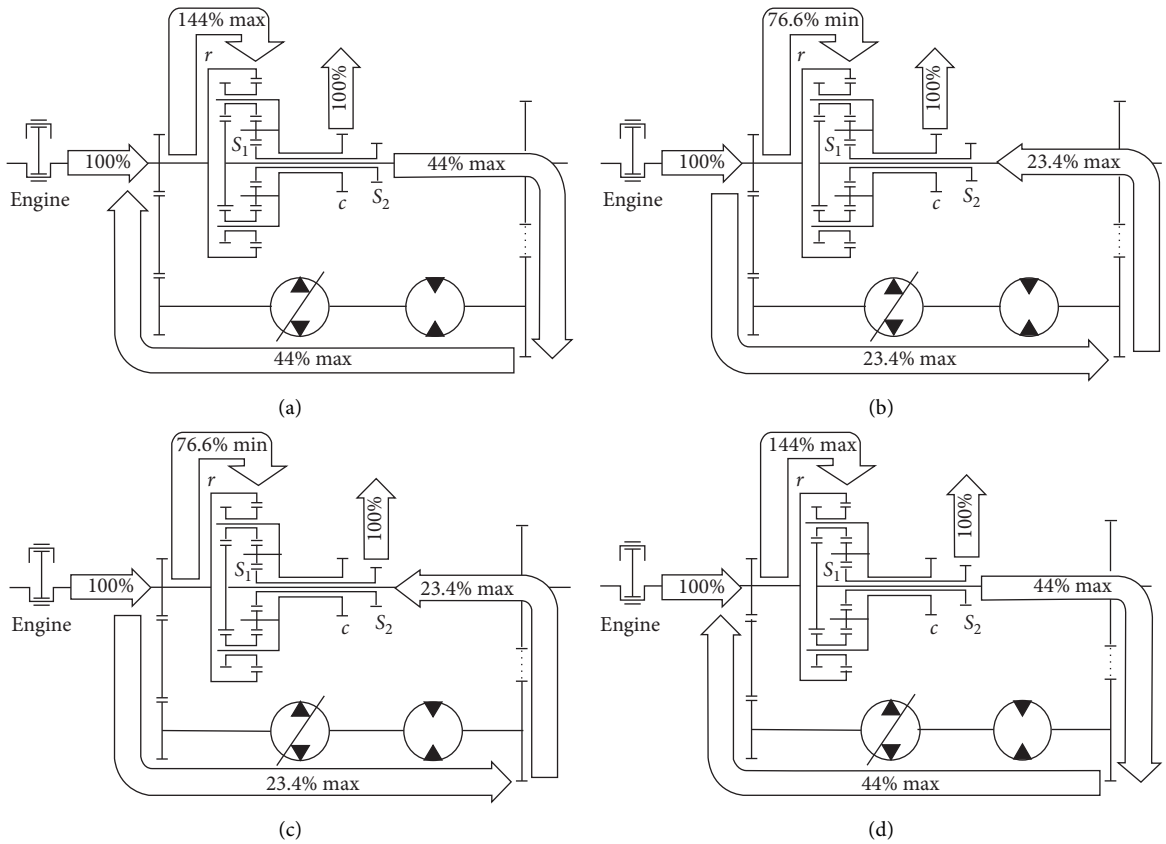

Figure 2: Power flow direction of the PGM of HMCVT. (a) Range HM1/HM3, $\varepsilon > 0$, power-circulation. (b) Range HM1/HM3, $\varepsilon < 0$, power-split. (c) Range HM2/HM4, $\varepsilon > 0$, power-split. (d) Range HM2/HM4, $\varepsilon < 0$, power-circulation.

Table 2: Equation of efficiency calculation for ranges HM1 and HM3.

Elements	Torque equation considering power losses			
	$\varepsilon > 0$		$\varepsilon < 0$	
	HM_1	HM_3	HM_1	HM_3
Engine	$T_e = T_r + \eta_1\eta_2 T_p / i_1 i_2$		$T_e = T_r + T_p / i_1 i_2 \eta_1 \eta_2$	
Pump	$T_p = \varepsilon \eta_H T_m$		$T_p = \varepsilon T_m / \eta_H$	
Motor	$T_m = \eta_3 T_{s_1} / (-i_3)$		$T_m = T_{s_1} / (-\eta_3 i_3)$	
PGM	$T_{s_1} + T_r + T_c = 0$			
PGM	$T_r = -k_1 T_{s_1} / \eta_{s_1 r}$			
Intermediate shaft	$T_c = T_z / i_4 i_8 \eta_4 \eta_8$	$T_c = T_z / i_4 i_7 \eta_4 \eta_7$	$T_c = T_z / i_4 i_8 \eta_4 \eta_8$	$T_c = T_z / i_4 i_7 \eta_4 \eta_7$
Output shaft	$T_z = T_o / (i_{11} i_{12} \eta_{11} \eta_{12})$			
Torque ratio	$\bar{\mu} = T_o / T_e$			
Efficiency	$\eta = -\bar{\mu} / i_g$			

When HMCVT is working in HM_1 or HM_3 range, if the transmission efficiencies of the gear pairs i_9 and i_8 are equal ($\eta_7 = \eta_8$), the transmission efficiencies of HMCVT in HM_1 and HM_3 ranges are equal.

When HMCVT is working in HM_2 or HM_4 range, if the transmission efficiencies of the gear pairs i_9 and i_6 are equal ($\eta_9 = \eta_6$), the transmission efficiencies of HMCVT in HM_2 and HM_4 ranges are also equal.

Due to the complexity of the above results, it is necessary to evaluate the influence of displacement ratio ε, standing transmission ratio of PGM $-k_1$, gear ratio $i_1 i_2 i_3$, and hydraulic system efficiency η_H on the transmission efficiency of HMCVT by means of image analysis method. We assume that $\eta_1 - \eta_{12}$ are 0.98, $\eta_{s_1 r}$ is 0.98, $\eta_{s_1 s_2}$ and $\eta_{r s_2}$ are 0.97, and $k_1 i_1 i_2 i_3$ is -3.2727. The evaluation results are shown in Figure 3.

According to the analysis on Figure 3, the following rules are obtained.

In each range of HMCVT, when the displacement ratio ε is 0, the transmission efficiency reaches the maximum value. Now the hydraulic path (HST) does not transmit power, and the power is completely transmitted by the mechanical path. When the displacement ratio ε is -1 or 1, the transmission efficiency reaches the minimum value, and the hydraulic

Table 3: Equation of efficiency calculation for ranges HM2 and HM4.

Elements	Torque equation considering power losses			
	$\varepsilon > 0$		$\varepsilon < 0$	
	HM_2	HM_4	HM_2	HM_4
Engine	$T_e = T_r + T_p/i_1 i_2 \eta_1 \eta_2$		$T_e = T_r + \eta_1 \eta_2 T_p/i_1 i_2$	
Pump	$T_p = \varepsilon T_m/\eta_H$		$T_p = \varepsilon \eta_H T_m$	
Motor	$T_m = T_{s_1}/(-\eta_3 i_3)$		$T_m = \eta_3 T_{s_1}/(-i_3)$	
PGM	$T_{s_1} + T_r + T_{s_2} = 0$			
PGM	$T_r = 1 - k_3 \eta_{s_1 s_2}/k_3 \eta_{s_1 s_2} - k_2 \eta_{rs_2} T_{s_2}$			
Intermediate shaft	$T_{s_2} = T_z/i_5 i_9 \eta_5 \eta_9$	$T_{s_2} = T_z/i_5 i_6 \eta_5 \eta_6$	$T_{s_2} = T_z/i_5 i_9 \eta_5 \eta_9$	$T_{s_2} = T_z/i_5 i_6 \eta_5 \eta_6$
Output shaft	$T_z = T_o/(i_{11} i_{12} \eta_{11} \eta_{12})$			
Torque ratio	$\tilde{\mu} = T_o/T_e$			
Efficiency	$\eta = -\tilde{\mu}/i_g$			

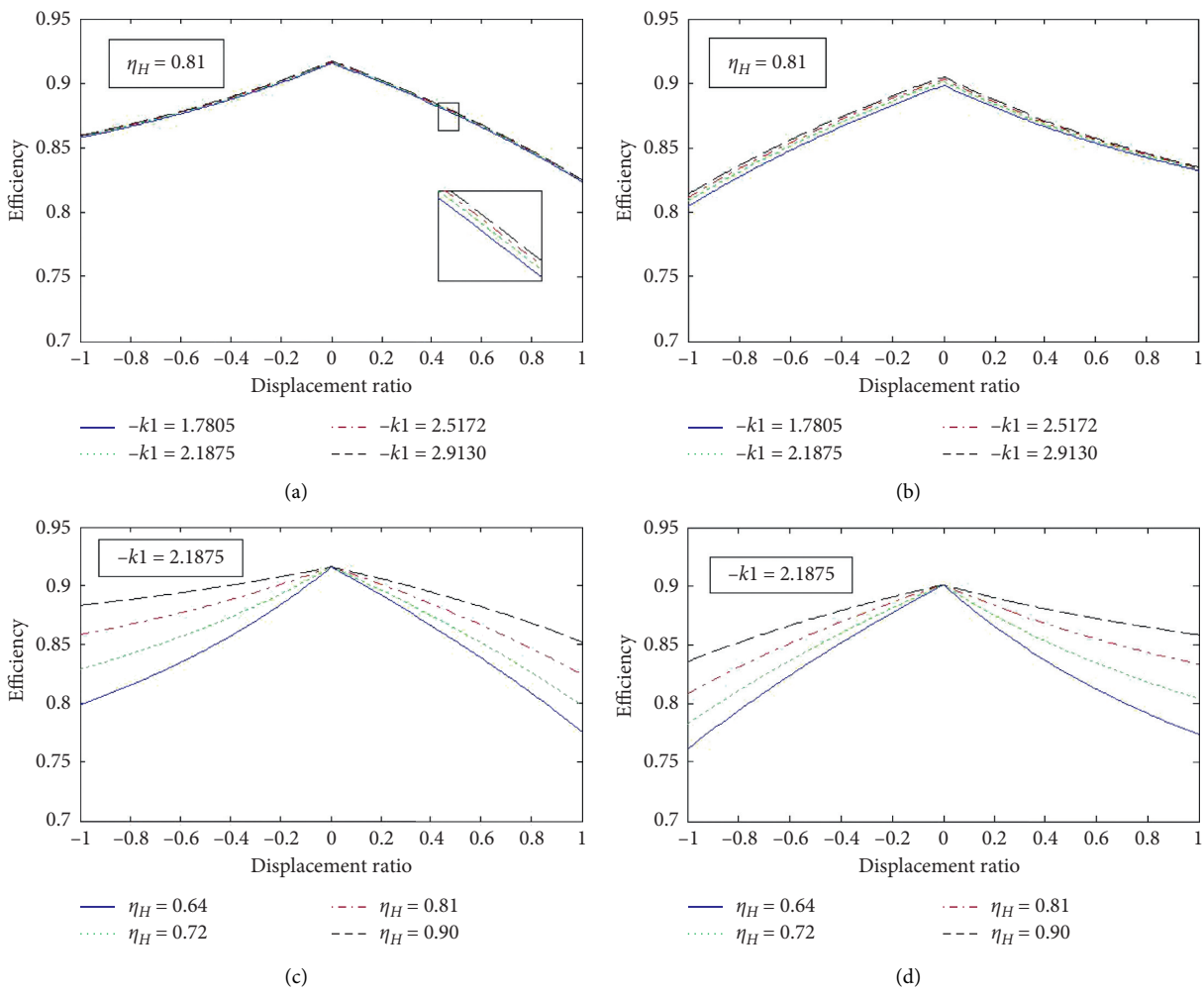

Figure 3: Continued.

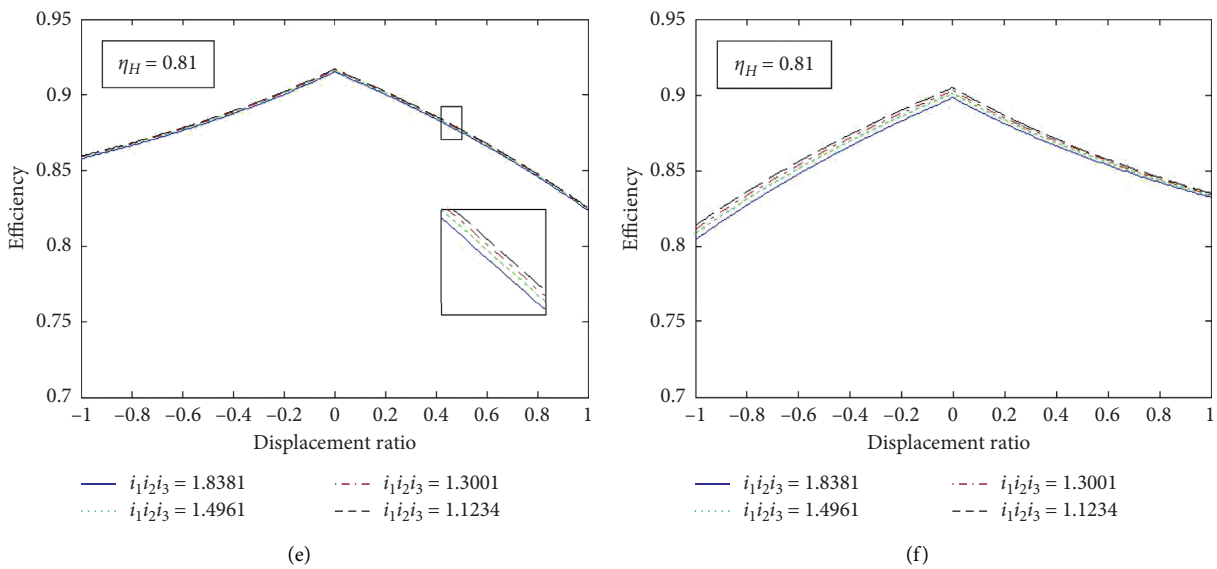

Figure 3: The influence of parameters on the transmission efficiency of HMCVT. (a) The influence of $-k_1$ on HM1 and HM3 ranges. (b) The influence of $-k_1$ on HM2 and HM4 ranges. (c) The influence of η_H on HM1 and HM3 ranges. (d) The influence of η_H on HM2 and HM4 ranges. (e) The influence of $i_1i_2i_3$ on HM1 and HM3 ranges. (f) The influence of $i_1i_2i_3$ on HM2 and HM4 ranges.

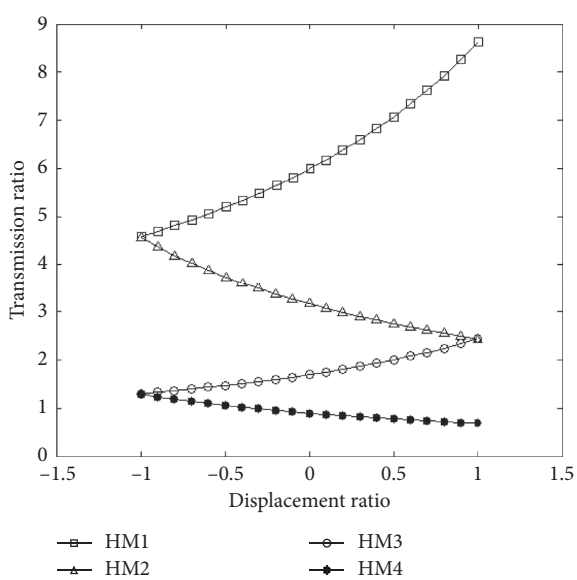

Figure 4: Relationship between transmission ratio and displacement ratio.

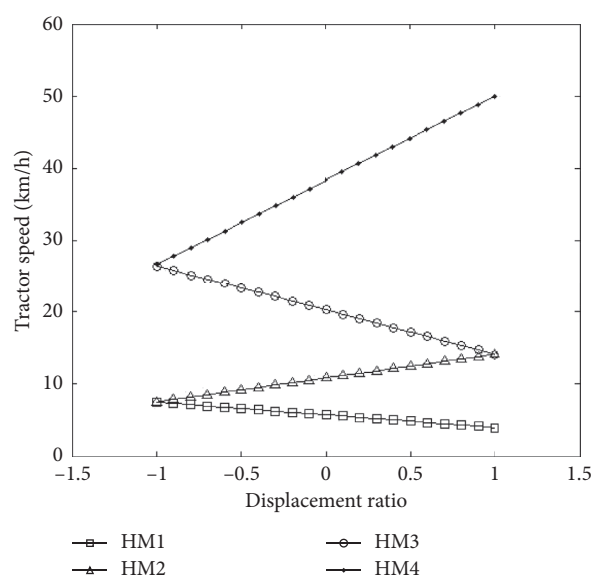

Figure 5: The curve of the tractor speed.

path transmits more power at this time, resulting in a lower overall efficiency of HMCVT.

In each range of HMCVT, the transmission efficiency value in the power circulation phase is lower than the transmission efficiency value in the power split phase, which indicates that the power circulation will cause the transmission efficiency of HMCVT to decrease.

The larger the value of the PGM standing transmission ratio $-k_1$, the higher the transmission efficiency of HMCVT, but the influence on improving the transmission efficiency is not obvious. The PGM standing transmission ratio $-k_1$ ranges from 1.5 to 3. The gear ratio $i_1i_2i_3$ and the PGM standing transmission ratio $-k_1$ are in an inversely proportional relationship; the smaller the value of the gear ratio $i_1i_2i_3$, the higher the transmission efficiency of HMCVT, and the influence on improving the transmission efficiency is also not obvious. The gear ratio $i_1i_2i_3$ ranges from 1.1 to 2.2.

The greater the value of HST efficiency η_H, the higher the overall transmission efficiency of HMCVT. The influence of η_H on improving transmission efficiency of HMCVT is significant.

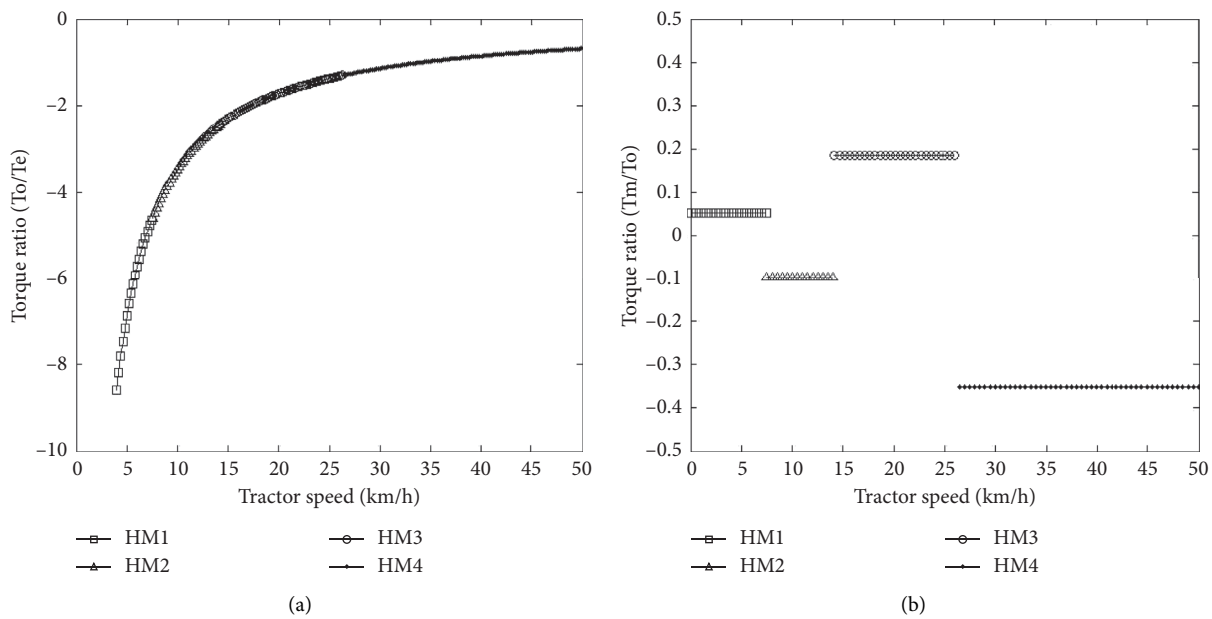

Figure 6: The curve of torque characteristic. (a) Ratios of output shaft torque to input shaft torque. (b) Ratios of motor shaft torque to output shaft torque.

5. Analysis on the Transmission Characteristics Results of HMCVT

According to the previous content, the value of the PGM standing transmission ratio $-k_1$ is set to 2.1875, and the HST efficiency value η_H is set to 0.81; then the other parameters of HMCVT are $k_2 = 0.2714$, $-k_3 = 0.5938$, $i_1 = i_2 = 1$, $i_3 = 1.5$, $i_4 = i_5 = 1$, $i_6 = 1.66$, $i_7 = 1.16$, $i_8 = 4.10$, $i_9 = 5.84$, and $i_{10} = i_{11} = i_{12} = 1$.

The relationship between the transmission ratio and displacement ratio is shown in Figure 4. The curve of the tractor speed is shown in Figure 5. In the first range, the displacement ratio changes from 1 to −1, the transmission ratio decreases from 8.62 to 4.59, and the tractor speed increases from 0 to 7.50 km/h. In the second range, the displacement ratio changes from −1 to 1, the transmission ratio decreases from 4.59 to 2.43, and the tractor speed increases from 7.50 km/h to 14.12 km/h. In the third range, the displacement ratio changes from 1 to −1, the transmission ratio decreases from 2.43 to 1.30, and the tractor speed increases from 14.12 km/h to 26.44 km/h. In the fourth range, the displacement ratio changes from −1 to 1, the transmission ratio decreases from 1.30 to 0.69, and the tractor speed increases from 26.44 km/h to 50 km/h. The results show that the stepless speed regulation of HMCVT in the tractor speed range of 0–50 km/h can be realized by the coordinated control of the HST displacement ratio and the clutches.

The ratios of the output shaft torque to the input shaft torque in each range of HMCVT are shown in Figure 6(a). The continuous change of torque can be realized in the entire working ranges. The ratios of the motor shaft torque to the output shaft torque in each range of HMCVT are shown in Figure 6(b). The torque ratio remains constant in each range and varies between different ranges. The values of torque ratios in the four ranges are 5.14%, −9.72%, 18.49%, and −35.18%, respectively.

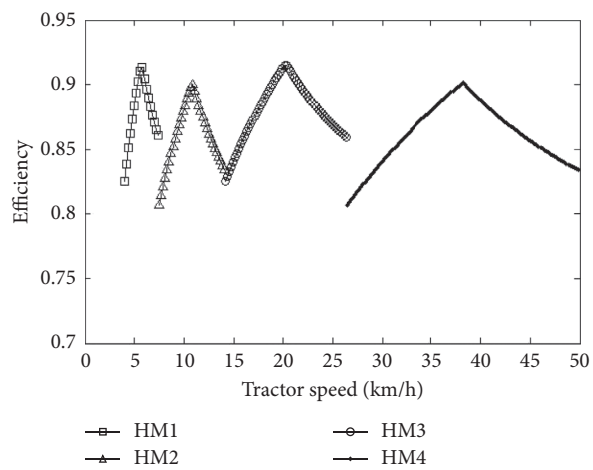

Figure 7: Overall transmission efficiency of HMCVT.

The relationship between the tractor speed and the overall transmission efficiency of HMCVT is shown in Figure 7. Each of the four ranges has a transmission efficiency maximum value of 0.917, 0.902, 0.917, and 0.902, respectively. The efficiency value always increases first with the increase of the tractor speed and then decreases after reaching the maximum value. The maximum transmission efficiency in each range is obtained when the HST displacement ratio is 0. Now, the hydraulic path does not transmit power and all power is transmitted by the mechanical path. The transmission efficiency of HMCVT is higher than 83%, so the overall transmission efficiency is at a high level.

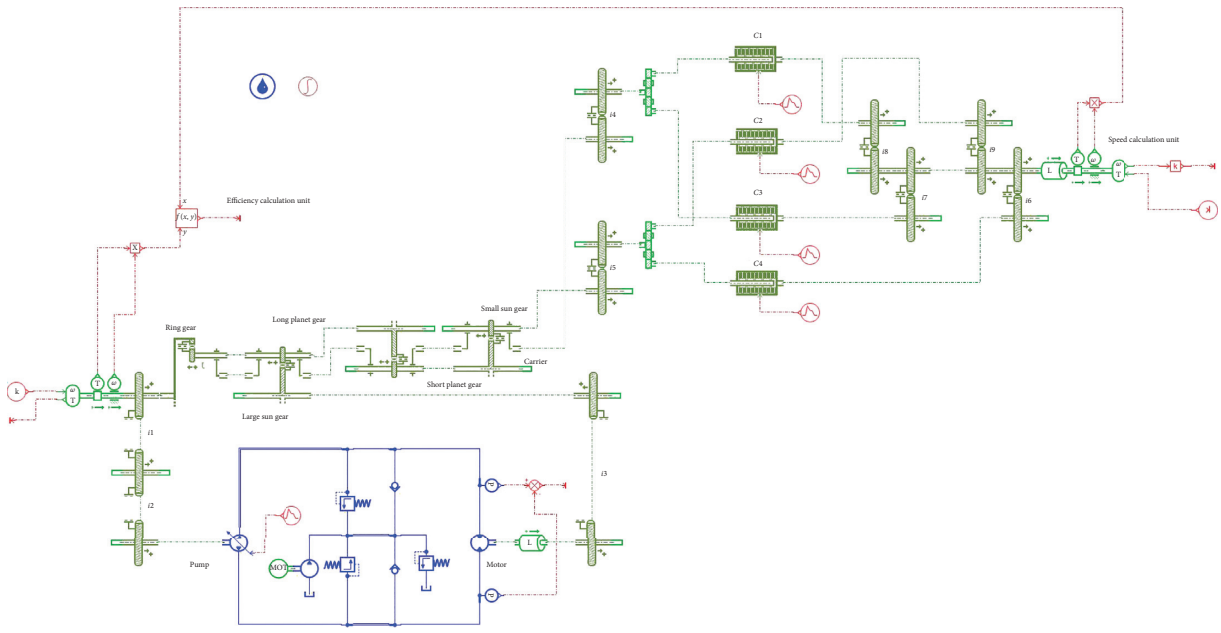

Figure 8: HMCVT simulation model.

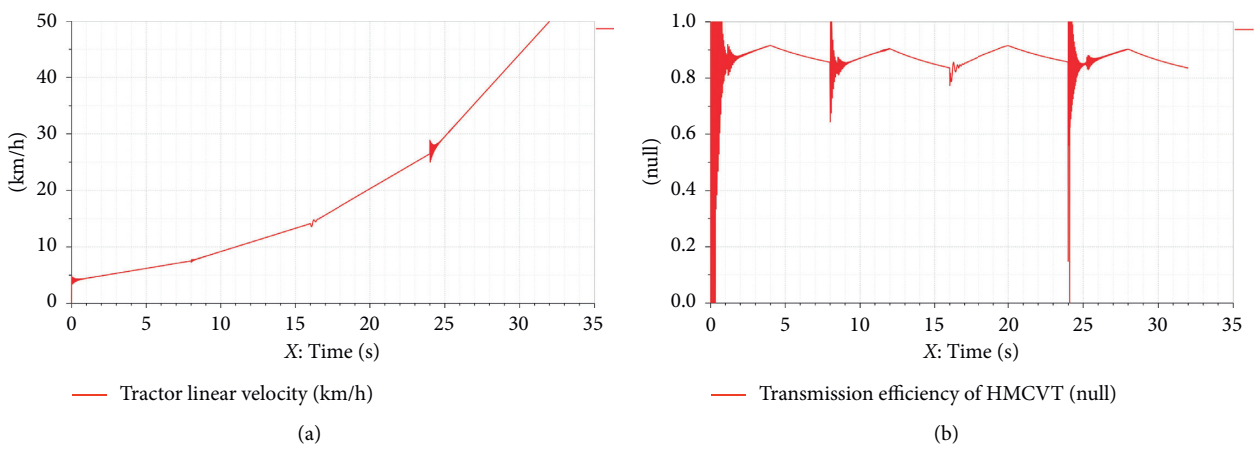

(a) (b)

Figure 9: Simulation results. (a) Simulation result of the tractor speed. (b) Simulation result of the transmission efficiency of HMCVT.

6. Verification of HMCVT Simulation Model

The modeling and simulation of HMCVT are accomplished by using Amesim simulation software. According to Figure 1, a simulation model of HMCVT is established, as shown in Figure 8.

6.1. Hydraulic System. The hydraulic system is mainly composed of a variable displacement hydraulic pump, a fixed displacement hydraulic motor, two relief valves, two check valves, and a charge hydraulic pump with a relief valve. The aim of the charge pump is to compensate for the leakage loss in the pipeline and to establish the lowest pressure in the pump's suction pipeline. Two relief valves are used to limit the maximum pressure in the system piping, and its adjustment pressure should be above the normal working pressure of the system. Volumetric losses of the pump and motor are neglected, and their hydromechanical efficiencies are set at 0.9.

6.2. Mechanical Components. Mechanical components are assumed to be constant efficiency components throughout the transmission. The power loss of each gear pair is 2%, so the efficiency is set to 0.98. In the Ravigneaux planetary gear mechanism, the efficiencies of ring gear-long planetary gear couple, long planetary gear-large sun gear couple, long planetary gear-short planetary gear couple, and short planetary gear-small sun gear couple are set at 0.99. The main reducer, differential, and wheel reducer are combined and modeled as a gear reducer with an efficiency of 0.965. To simplify the model, the friction losses of the shaft, gears, and bearings were ignored during the simulation modeling process.

6.3. Model Control and Simulation Results. The engine speed is assumed to have a constant value of 2200 r/min; the load torque of the output shaft of HMCVT is set to 100 Nm; the model simulation time is 32 s, including range HM_1: 0–8 s, range HM_2: 8–16 s, range HM_3: 16–24 s, and range HM_4: 24–32 s.

The simulation results are shown in Figure 9; through the variable pump displacement and coordinated control of the clutches [18, 19], the transmission gradually changes from range HM_1 to range HM_4, and the tractor achieves stepless speed change from 0 to 50 km/h. The simulation results are consistent with the previous theoretical analysis results, which show that the 4-range HMCVT transmission scheme proposed in this paper is suitable for matching wheeled tractors.

6.4. Comparison. Xu LY's transmission scheme [15] has been applied to mass production tractors. This transmission scheme has 6 working ranges in the forward direction and 3 working ranges in the reverse direction, which is controlled by 8 clutches. The speed range in the forward direction is 0~30 km/h, while the reverse direction is only 0~10 km/h. The transmission efficiency of the hydraulic range is low (less than 80%); the transmission efficiency of the hydromechanical ranges is high (higher than 90%) but is only in the forward direction.

The scheme proposed in this paper has 4 working ranges and a speed range of 0~50 km/h in the forward and reverse directions, which is controlled by 6 clutches. The fewer the transmission ranges, the less switching during the working ranges, so the transmission performance is improved. The smaller number of clutches ensures that the system is easier to control. The transmission efficiencies in the forward and reverse directions are close, the overall forward transmission efficiency is higher than 83%, and the highest transmission efficiency is higher than 91%.

Therefore, the application of HMCVT proposed in this paper is wider; it can not only match conventional tractors but also match two-way operation tractors and other engineering vehicles.

7. Conclusions

This paper proposes a new type of transmission scheme of HMCVT. The Ravigneaux PGM and the HST are connected in parallel to form a closed loop and then connected in series with the range switching mechanism. This new HMCVT features a double-row PGM with 4 hydromechanical working ranges. By coordinating control of the HST displacement ratio and the engagement conditions of shifting clutches, the stepless speed regulation of HMCVT at the tractor speed of 0–50 km/h is realized.

According to the theoretical analysis on the new HMCVT, the speed characteristic curve and the torque characteristic curve are obtained. Based on the power flow direction of HMCVT, the transmission efficiency curve is obtained by using the Крейнес formula.

Using image analysis method to study the influence of four parameters (displacement ratio ε, PGM standing transmission ratio $-k_1$, gear ratio $i_1 i_2 i_3$, and hydraulic system efficiency η_H) on the transmission efficiency of HMCVT, the results show that the standing transmission ratio $-k_1$ and gear ratio $i_1 i_2 i_3$ have little effect on the transmission efficiency, whereas the displacement ratio ε and hydraulic system efficiency η_H have a greater impact on the transmission efficiency.

The parameters of the new HMCVT are finally determined. The results of the transmission characteristics show that the new HMCVT proposed in this paper has the stepless speed regulation capability for tractors, which can also continuously transmit and change the torque. The transmission efficiency of HMCVT is at a high level.

In order to verify the theoretical derivation, Amesim simulation software is used for the modeling and simulation of HMCVT. The simulation results are consistent with the theoretical analysis results. Therefore, we believe that the transmission scheme is reasonable and effective for tractors.

Data Availability

The Simcenter Amesim System File data used to support the findings of this study are available from the corresponding author upon request.

Conflicts of Interest

The authors declare that they have no conflicts of interest.

Acknowledgments

This research was financially supported by the National Key Research and Development Plan Project of China (2016YFD0700402) and Changzhou Sci & Tech Program (no. CE20185037).

References

[1] L. Y. Xu, Z. L. Zhou, M. Z. Zhang et al., "Research and design of hydro-mechanical continuously variable transmission for tractors," *Journal of Northeast Agricultural University*, vol. 13, no. 2, pp. 182–186, 2006.

[2] R. Paoluzzi and L. G. Zarotti, "The minimum size of hydrostatic transmissions for locomotion," *Journal of Terramechanics*, vol. 50, no. 3, pp. 153–164, 2013.

[3] J. Kim, J. Kang, Y. Kim, B. Min, and H. Kim, "Design of power split transmission: design of dual mode power split transmission," *International Journal of Automotive Technology*, vol. 11, no. 4, pp. 565–571, 2010.

[4] A. Kim and A. Rossetti, "Fuel consumption reduction in urban buses by using power split transmissions," *Energy Conversion and Management*, vol. 71, pp. 159–171, 2013.

[5] A. Rossetti and A. Macor, "Multi-objective optimization of hydro-mechanical power split transmissions," *Mechanism and Machine Theory*, vol. 62, pp. 112–128, 2013.

[6] A. Macor and A. Rossetti, "Optimization of hydro-mechanical power split transmissions," *Mechanism and Machine Theory*, vol. 46, no. 12, pp. 1901–1919, 2011.

[7] S. Shamshirband, D. Petković, A. Amini et al., "Support vector regression methodology for wind turbine reaction torque prediction with power-split hydrostatic continuous variable transmission," *Energy*, vol. 67, pp. 623–630, 2014.

[8] K. T. Anuar, "Resch R Continuously variable tractor transmissions," *ASAE Distinguished Lecture No. 29*, pp. 1–37, St. Joseph: American Society of Agricultural Engineers, St Joseph, MI, USA, 2005.

[9] S. H. Yuan and J. B. Hu, "The efficiency of multi-range hydromechanical stepless transmission," *Journal of Beijing Institute of Technology*, vol. 7, no. 2, pp. 129–133, 1998.

[10] X. J. Liu, *Analysis of Vehicle Transmission System*, pp. 258-259, National Defence Industry Press, Beijing, China, 1998.

[11] M. M. Brenninger, "Fendt vario CVT in agricultural tractors," SAE International, Warrendale, PA, USA, SAE Technical Paper 2007-01-4205, 2007.

[12] H. Aitzetmüller, "Steyr S-Matic-the future CVT system," in *Proceedings of the Seoul 2000 FISITA world automotive congress*, pp. 1–6, Seoul, South Korea, June 2000.

[13] J. Pohlenz and K. Grad, "CVT for input power above 300 kW," *VDI-berichte*, vol. 2007, pp. 59–65, 2001.

[14] J. Pohlenz and K. Grad, "CVT-System für den Großflächeneinsatz," *VDI-berichte*, vol. 2004, pp. 23–33, 1855.

[15] L. Y. Xu, *Study on Characteristics of Hydro-Mechanical Continuously Variable Transmission of Tractor*, Xi'an University of Technology, Xi'an, China, 2007.

[16] J. Looman, *Zahnradgetriebe-Grundlagen, Konstruktionen, Anwendungen in Fahrzeugen*, Springer, Berlin, Germany, 2009.

[17] Z. Rao, *Planetary Gear Transmission Design*, Chemical Industry Press, Beijing, China, 2003.

[18] X. Xu, Y. Liang, M. Jordan, T. Peter, and D. Peng, "Optimized control of engine start assisted by the disconnect clutch in a P2 hybrid automatic transmission," *Mechanical Systems and Signal Processing*, vol. 124, 2019.

[19] S. Wang, Y. Liu, Z. Wang et al., "Adaptive fuzzy iterative control strategy for the wet-clutch filling of automatic transmission," *Mechanical Systems and Signal Processing*, vol. 130, pp. 164–182, 2019.